universität wien

MASTERARBEIT / MASTER´S THESIS

Titel der Masterarbeit / Title of the Master´s Thesis

Predicting nicotine-related craving in smokers from fMRI data using multivariate pattern analysis

verfasst von / submitted by

Lisa-Maria Neuner, B.Sc.

angestrebter akademischer Grad / in partial fulfilment of the requirements for the degree of

Master of Science (MSc)

Wien, 2021 / Vienna 2021

Studienkennzahl lt. Studienblatt / degree programme code as it appears on the student record sheet:	UA 066 840
Studienrichtung lt. Studienblatt / degree programme as it appears on the student record sheet:	Masterstudium Psychologie UG2002
Betreut von / Supervisor	Univ.-Prof. Dr. Frank Scharnowski, MSc

Table of contents

Abstract

Nicotine addiction is a leading cause of preventable death worldwide and leads to high costs for health systems. Unfortunately, relapse rates after smoking cessation are high, which calls for improved treatment options. To deliver new effective treatments, a better understanding of the neural and behavioral mechanisms underlying nicotine dependence is needed. Regarding the neural underpinnings of nicotine addiction, a recent study found that activity in the anterior cingulate cortex may be primarily related to cue-driven craving, while amygdala activity is associated with valence aspects of nicotine cues. This work examined possible confounding of valence with craving using a cue-reactivity paradigm. 32 nicotine dependent subjects underwent a functional magnetic resonance imaging session while viewing craving-inducing images and subsequently rated these on a continuous scale regarding urge-to-smoke and emotional valence. A machine learning model (LASSO-PCR) was applied to predict single-trial ratings from neuronal activity in the anterior cingulate cortex. We hypothesized successful predictions only for the craving ratings, but it was not possible to accurately predict craving nor valence. The results can be attributed to various factors: quality of the ratings, unsuitable inter-stimulus interval, and the model itself. Overall, optimizing experimental designs for multivariate regression methods is highly relevant to enhance research on cue-related craving in smokers and thus to develop better treatment options for smoking cessation.

Keywords: craving, cue-reactivity, nicotine dependence, functional magnetic resonance imaging, machine learning

Introduction

With more than 8 million deaths per year worldwide (World Health Organization, 2021), tobacco use disorder is one of the main preventable diseases (Samet, 2013). The cost on the global health system has been estimated to $1.4 trillion per year (World Health Organization, 2021), which makes cigarette smoking not only a major threat to public health, but also a huge burden to socioeconomic systems. It is not surprising that nearly 70% of smokers want to quit (Babb et al., 2017), but they often fail to stay abstinent, as illustrated by relapse rates of around 50% in the first year of smoking cessation (García-Rodríguez et al., 2013). Several treatments are available, such as cognitive behavioral therapy, medication, or nicotine replacement products like nicotine patches, nicotine gum, and sprays. However, these treatments show poor efficacy (Quednow & Herdener, 2016). For example, nicotine replacement therapy and individual behavioral counseling increase the success of smoking cessation in the first six months by only 3% (Hartmann-Boyce et al., 2018; Lancaster & Stead, 2017). Consequently, it is urgently needed to improve existing treatment options and develop new approaches.

Understanding the associated behaviors and underlying mechanisms involved in the development and maintenance of nicotine addiction is essential to achieve this goal. Here, several psychological factors for smoking relapse have been identified, including impulsivity (Powell et al., 2010), sociability (Nieva et al., 2011), perceived stress (Nakajima & Al'Absi, 2012), and low self-efficacy (Elfeddali et al., 2012).

Craving also appears to be a key factor for relapse (Bagot et al., 2007; Killen & Fortmann, 1997; Nakajima & Al'Absi, 2012). Defined as "persistent urges, thoughts or desires to smoke a cigarette" (Potvin et al., 2015), craving is one core diagnostic criterion for tobacco use disorder according to the *Diagnostic and Statistical Manual of Mental Disorders 5th Edition* (DSM-V; American Psychiatric Association, 2013). Different theories on addiction, based on basic learning models, have attempted to explain why craving arises.

Models of addiction

Addiction models based on classical conditioning (Pavlov, 1927) postulate that the repeated pairing of certain stimuli (environmental context or drug paraphernalia) with drug use leads to craving being triggered by the stimuli alone, as a pleasant state is expected, but not yet achieved (Tiffany, 1995). For example, if a smoker has always smoked a cigarette when drinking coffee in the morning, a coffee cup may trigger craving.

In contrast, withdrawal-based negative reinforcement models focus on physical dependence and instrumental conditioning (Skinner, 1963), and propose that the frequency of a particular behavior increases if it prevents an undesirable consequence. Here, addiction is explained as maintaining drug use to avoid unpleasant withdrawal symptoms, like anxiety or restlessness in smoking cessation (Eissenberg, 2004; Tiffany, 1990). Thus, certain cues may lead to craving because they are associated with the aversive situation of withdrawal (Betts et al., 2021).

The incentive sensitization theory (Robinson & Berridge, 1993) attempts to explain craving at the neurobiological level. The core assumption is that repeated exposure to addictive substances induces permanent changes in brain circuits that are typically responsible for associating incentives with stimuli. Consequently, the substance user becomes hypersensitive to drug cues, which influences motivation (wanting) and leads to explicitly observable behavior such as craving.

All these models share the assumption that craving can be triggered because of newly learned associations. Thus, craving is highly driven by the environment and external stimuli frequently associated with drug use, or in other words, by drug cues (Betts et al., 2021). Since smokers constantly encounter such craving-inducing situations that might prevent smoking cessation, it is important to further examine this mechanism in detail. One approach to study cue-driven craving is the cue-reactivity paradigm (Carter & Tiffany, 1999; Drummond et al., 1995).

Cue-reactivity paradigm

The cue-reactivity paradigm is a method used in laboratory settings to examine physiological responses to certain stimuli in contrast to neutral cues. In studies on nicotine addiction, subjects are shown smoking cues, for example images of cigarettes (Carter & Tiffany, 1999; Ferguson & Shiffman, 2009), and the response of interest is measured simultaneously or subsequently. Here, craving assessment can be done with visual analog scales (Hughes, 1992), while physiological proxies for craving can include measurements of heart rate and skin conductance (Tong et al., 2007).

However, combining the cue-reactivity paradigm with functional magnetic resonance imaging (fMRI) allows to identify neural correlates of craving (Chase et al., 2011; Kühn & Gallinat, 2011; Tang et al., 2012). Interestingly, it was found that brain activity during exposure to smoking cues was predictive of smoking cessation and relapse (Allenby et al., 2020; Janes et

al., 2010). These findings highlight that understanding the underlying neural mechanisms of nicotine dependence and craving is highly relevant for improved treatments.

Neural underpinnings of addiction

The following brain regions have been consistently identified in meta-analyses to be active during cue exposure in individuals with drug addiction: ventral striatum, amygdala, anterior cingulate cortex (ACC), posterior cingulate cortex, and orbitofrontal cortex (Chase et al., 2011; Kühn & Gallinat, 2011; Tang et al., 2012).

For example, the ventral striatum, which includes the nucleus accumbens, is highly involved in reward-based processing and learning (Daniel & Pollmann, 2014) and therefore plays an important role in substance dependence. Although the amygdala is known primarily for processing emotions (Gallagher & Chiba, 1996), it is also active in learning associations between cues and rewards (Baxter & Murray, 2002), thus promoting drug seeking and cue-induced relapse (See et al., 2006). In addition, the orbitofrontal cortex, which is connected to the amygdala and the nucleus accumbens, appears to be particularly involved in evaluating the incentive value of stimuli and is consequently also a key region for reward processing in addiction (Gottfried et al., 2003; Schoenbaum et al., 2006).

Regarding cue-driven craving, several studies found a strong involvement of the ACC (Brody et al., 2007; Canterberry et al., 2013; Kühn & Gallinat, 2011; Li et al., 2013). This region is part of higher-level executive functions such as reward-based decision-making (Bush et al., 2002) and impulse control (Simmonds et al., 2008). Here, for example, top-down control is exerted on the ventral striatum (Kalivas & Volkow, 2005). In contrast, the posterior cingulate cortex, as part of the default mode network, has a more indirect role and was found to be active in resisting cue-driven craving (Brody et al., 2007).

However, recent studies on nicotine dependence suggested that distinct psychological aspects of the stimuli were supported by different neural substrates. For instance, ACC activity was found to be correlated with craving but not with valence of presented smoking images (Haugg et al., 2021). Additionally, the amygdala has been associated with the processing of affective stimuli (Costafreda et al., 2008), while also found to be substantially involved in cue-reactivity studies on addiction (Kühn & Gallinat, 2011). These findings indicate that other dimensions like the emotional aspect may confound with results on craving-associated brain activity. This particularly concerns studies using the cue-reactivity paradigm to examine craving

at the neural level, since it cannot be ruled out that observed brain response was induced by psychological aspects of the cues other than craving.

In addition, this issue is critical for specific treatments for smoking cessation such as cue-exposure therapy (Conklin & Tiffany, 2002; Drummond et al., 1990) and real-time fMRI neurofeedback (Cox et al., 1995; Sulzer et al., 2013). In these treatments, clinicians aim to reliably induce craving rather than valence using smoking cues. Furthermore, in real-time fMRI neurofeedback, it is essential to target the right brain region responsible for craving to provide accurate feedback.

Consequently, it is highly relevant to determine precisely which brain regions respond to the craving- or valence-related component of images shown to further improve studies using the cue-reactivity paradigm as well as treatments for smoking cessation.

Approach in this study

This work consists in re-analyzing an in-house fMRI data set, which was published in the paper by Haugg et al. (2021) on disentangling different psychological dimensions of craving-inducing cues at the brain level.

For this purpose, 32 smokers were exposed to a cue-reactivity paradigm while undergoing fMRI scanning. Afterwards, the participants rated the images regarding urge-to-smoke (craving) and emotional perception (valence) on a visual 0-100 analog scale.

We attempt to verify the findings of Haugg et al. (2021) on the association of ACC activity with the craving rather than the valence aspect of stimuli. More precisely, while Haugg et al. (2021) used a classical univariate model with ratings as parametric modulator, we chose to apply a cross-validated multivariate approach at the single-trial level. Classical methods often underestimate the amount of information that can be extracted from neuroimaging data (Haynes & Rees, 2006). The reason is that the difference in activity of distinct neuronal processes can be very small and only be detected by combining several voxels instead of one to find patterns of activation. Furthermore, cross-validation (Kohavi, 1995) provides information on whether a model can be generalized beyond the data set used for the analysis. This is particularly important for real-time fMRI neurofeedback, where feedback must be given on unseen cases.

We expect to find a machine learning model that accurately predicts craving ratings from BOLD activity in the ACC. Furthermore, we expect that it is not possible to accurately predict the valence ratings from this region.

Methods

The data was acquired at the University of Zurich and taken from Haugg et al. (2021) to be reanalyzed for this thesis.

Participants

The sample consisted of 32 participants (female = 16, male = 15, non-binary = 1; age: *M* = 25.93, *SD* = 5.30; average daily cigarette consumption in number of cigarettes: *M* = 11.47, *SD* = 5.57; smoking duration in years: *M* = 7.41, *SD* = 4.76). All subjects provided written consent and received compensation for their participation in the form of 25 Swiss francs per hour. Only individuals with tobacco use disorder as defined in the DSM-V (American Psychiatric Association, 2013) were included. In addition, these exclusion criteria applied: mental or neurological disorders, contraindications for an MRI examination (metal implants, present pregnancy, pacemaker, etc.), and use of non-cigarette tobacco substitutes (e.g., nicotine patches, chewing gums, electronic cigarettes).

Experimental procedure and design

Before the MRI scan, subjects had to complete the following questionnaires: anamnesis questionnaire of current and past drug use (described in Quednow et al., 2004), Fagerström Test for Nicotine Dependence (Heatherton et al., 1991), and Brief Questionnaire of Smoking Urges (QSU; Sanderson Cox et al., 2001). The QSU had to be filled out again after the MRI. In addition, we instructed the participants not to smoke for at least one hour prior to the appointment.

An event-related parametric design was employed for the MRI session, in which participants were asked to view a total of 330 nicotine-related and neutral images passively. There were five runs, each lasting five minutes. 68 images were shown randomly for 2.3 seconds each during one run, followed by a 1-second fixation point to set the baseline. Additionally, a 15-second fixation point baseline was displayed at the beginning of each run. Furthermore, to ensure that participants were attentive to the images, we included ten catch trial images in random order. These were indicated by an exclamation mark, and subjects were asked to press a button each time it appeared. Before and after the cue-reactivity task, we collected resting state scans, which required the subjects to fixate a white dot on a black background for seven minutes each. At the end of the session, we acquired an anatomical image in addition to the functional images. One session lasted about 50 minutes in total.

The images (examples shown in Figure 1) induced very mild to very intense nicotine-craving, which was validated in another study (Manoliu et al., 2021). They were taken from the following databases: Smoking Cue Database (SmoCuDa; Manoliu et al., 2021), International Smoking Image Series (ISIS; Gilbert & Rabinovich, 1999), and International Affective Picture System (IAPS; Lang et al., 1997).

Following the scan, participants rated the total of 330 images shown using a 100-point visual analog scale. These were displayed randomly and had to be rated regarding the urge to smoke when viewed (craving) and how positively or negatively they were perceived (valence).

Figure 1

Examples of Different Types of Craving-Inducing Images Used in the Study

Image acquisition

Imaging was performed at the MR Center of the Psychiatric University Hospital in Zurich, Switzerland, using a 3 Tesla Philips Achieva scanner (Philips Healthcare, The Netherlands) with a 32-channel head coil. The passive viewing runs lasted 4:18 minutes, during which five dummy scans and 122 functional images were acquired with the following setup: T2*-weighted gradient-echo planar imaging (EPI) sequence with echo time (TE) = 35 ms, repetition time (RT) = 2000ms, 27 slices in ascending order, interslice gap = 1mm, flip angle (FA) = 82°,

voxel size = 2 x 2 x 3 mm3, and field of view (FoV) = 220 x 220 x 109 mm3. The subsequent anatomical scan lasted 8:26 minutes and was performed using this setup: T1-weighted sequence, FA = 8°, 237 sagittal slices in ascending order, no slice gap, voxel size = 0.76 x 0.76 x 0.76, and FoV = 255 x 255 x 180 mm3.

fMRI analysis

Overview

The fMRI analysis consisted of the following steps: (1) Preprocessing; (2) Trial-by-trial deconvolution: Generation of single-trial brain activity maps for each subject; (3) Feature selection: Application of an a priori mask (4) Implementation of a cross-validated machine learning model to predict craving ratings; (5) Permutation for model performance assessment; (6) Bootstrapping to threshold most reliable voxel weights for visualization and interpretation. Steps (4) to (6) were repeated using the valence ratings as a predictor. For an overview of the analysis process see Figure 2.

MRI processing and analyses were conducted with MATLAB R2021a (The MathWorks, Natick, USA) and Statistical Parametric Mapping (SPM12; Wellcome Trust Centre for Neuroimaging, London, United Kingdom). For preprocessing, we used the SPM12-based CONN toolbox (Whitfield-Gabrieli & Nieto-Castanon, 2012) and applied their default preprocessing pipeline. The deconvolution was based on SPM12 using a custom script. Machine learning analysis, model performance assessments, and visualizations were performed with the CanlabCore toolbox (Wager, 2021).

Figure 2

Visualization of the Whole Analysis Process

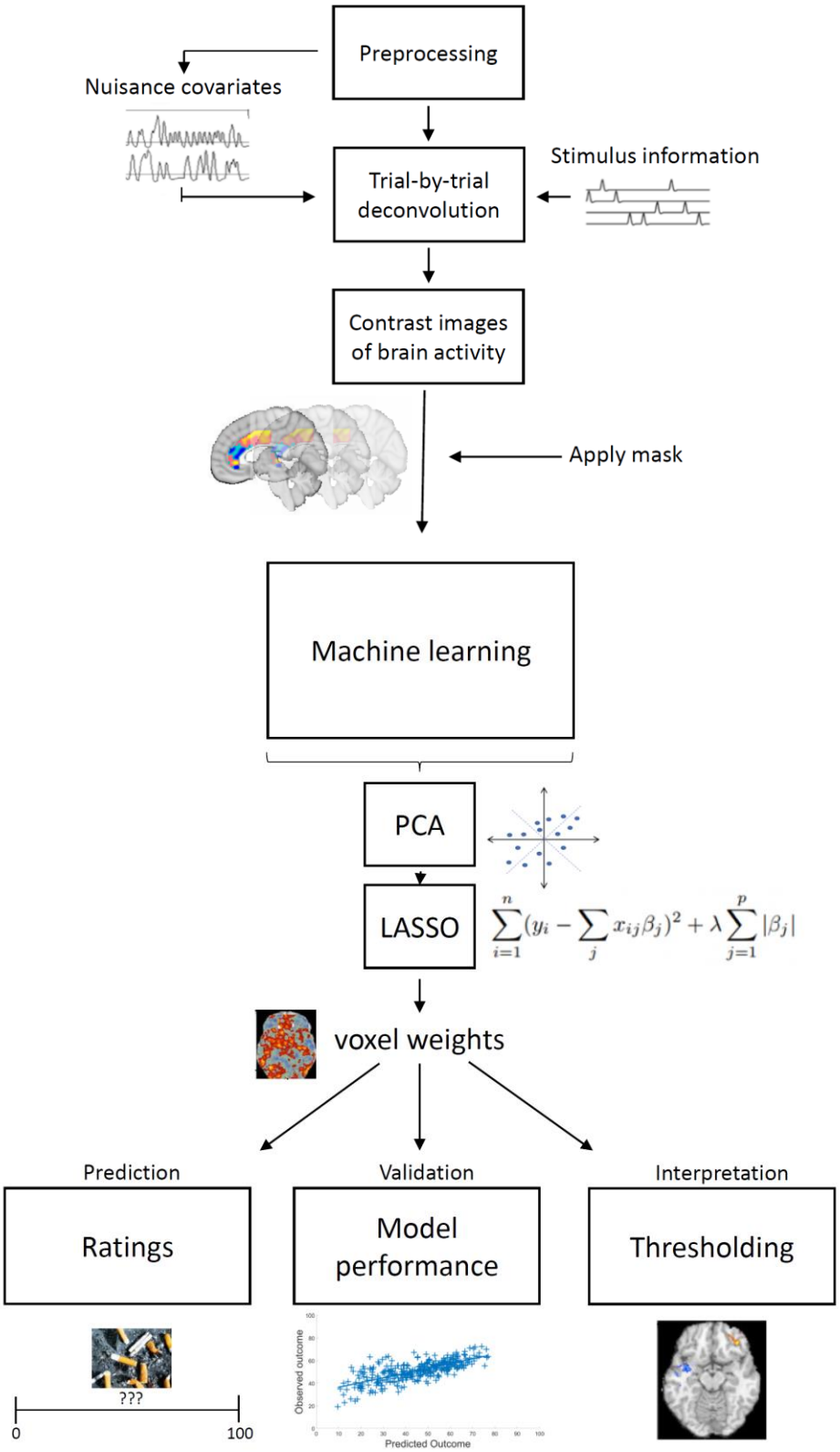

Note. Partially adapted from Wager et al. (2011; 2013).

Preprocessing

The following preprocessing steps were performed on the MRI images: realignment (six-parameter, rigid-body transformation), co-registration (of functional images to the anatomical image), slice-timing-correction (to account for inter slice differences in acquisition time), outlier detection (labeling images with frame-related shifts above 0.9 millimeter or global BOLD signal changes above five standard deviations), segmentation, normalization into Montreal Neurological Institute (MNI) space, smoothing with a 6 mm full-width-at-half-maximum (FWHM) Gaussian kernel.

Trial-by-trial deconvolution

A classical general linear model (GLM) was specified to generate contrast images of brain activity for every single subject, which were later taken as input for the machine learning analysis. For deconvolution of BOLD activity, we used the Least Squares-Separate approach (LS-S; Mumford et al., 2012). Here, the trial-by-trial beta values (regression slopes) for every voxel were estimated by treating one trial as the regressor of interest, while all others were included as one single nuisance regressor. Through this procedure, contrast images were obtained for every participant, which contained beta values for each voxel. The LS-S method has been shown to provide the best estimate of the true activity magnitude in event-related designs for multivoxel pattern analysis, for example regarding the signal-to-noise ratio (Mumford et al., 2012).

Additionally, the following covariates were modeled as regressors of no interest in the GLM: catch-trials, six motion parameters (based on estimated movement during realignment), and estimated outlier images.

Furthermore, the dataset was randomly downsampled to 180 trials per subject (5760 in total) for computational efficiency.

Feature selection

An anatomical mask of the ACC (see Figure 3) from the Harvard-Oxford atlas was applied to the brain images, which contained a total of 2500 2 mm^3 voxels for the analysis. The selection was based on previous studies that associated this region with cue-driven craving in smokers (Chase et al., 2011; Haugg et al., 2021; Kühn & Gallinat, 2011; Tang et al., 2012).

Figure 3

Illustration of the Anterior Cingulate Cortex

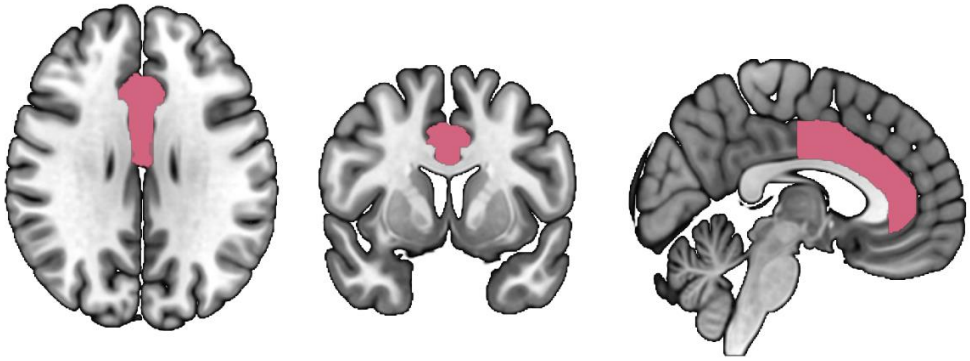

Note. Horizontal, coronal, and sagittal view of the brain with the anterior cingulate cortex marked in pink.

Machine learning algorithm

The term machine learning (ML) in fMRI data analysis refers to methods that use algorithms to infer mental states from patterns of neural responses (Haxby, 2012; Haynes & Rees, 2006). For this work, ML was applied to decode the participants' urge to smoke (craving) from their BOLD activity. A model based on *least absolute shrinkage and selection operator-regularized principal component regression* (LASSO-PCR; Wager et al., 2011) was chosen. The previously generated contrast maps were converted into a single vector and served as predictors, while the average craving ratings were specified as the outcome variable.

LASSO-PCR is a technique combining LASSO (Hastie et al., 2009; Tibshirani, 1996) regression with principal component analysis (PCA). Thereby, PCA was used as a first step. Here, we decided to retain the size of observations (N = 32) as number of components, in accordance with Chang et al. (2015). Afterwards, LASSO regression was applied to the resulting component scores to predict the ratings. More precisely, LASSO shrinks beta values (regression slopes) towards zero using a regularization term with a weight parameter (λ, lambda) that penalizes high coefficients and eliminates them. Lambda is a so-called *hyperparameter* and must be tuned (see section on cross-validation). The whole procedure resulted in a pattern of regression weights that were used for the prediction and visualization.

LASSO combined with PCA offers several advantages (Wager et al., 2011). First, in fMRI analysis we are dealing with very high dimensional data and thus with the *curse of dimensionality* (Bellman, 2015). This means that a high number of features (here: every single

voxel) in relation to the sample size reduces the prediction accuracy. Additionally, voxels are interdependent because they function in networks and should therefore not be treated separately. PCA addresses both issues because it reduces the amount of data by identifying and grouping of networks that are highly correlated with each other while preserving statistically relevant information. The LASSO algorithm then further removes components that are unstable and do not contribute to the prediction, leaving only the most useful ones. Overall, this combination provides a simplified model and facilitates the interpretation as well as visualization of the results (Hastie et al., 2009; Wager et al., 2011).

Cross-validation

One problem of ML methods is that they base their prediction on both true effects and noise of the data collected. The model therefore knows the learned data very well and shows good predictive performance, but cannot be applied to new, unseen cases – it suffers from *overfitting* (James et al., 2013). The common solution to overcome this problem is cross-validation (CV; Kohavi, 1995). In our case a special form of *k*-fold-CV was used, where the number of folds equals the number of observations ($k = N = 32$), referred to as CV1. Furthermore, the optimal lambda (regularization parameter of LASSO regression) that minimizes the prediction error (PE) was estimated in an additional *k-1*-fold CV, referred to as CV2.

The implementation of this so-called nested CV prevents *data leakage* when training the model and choosing the hyperparameter, otherwise information from the hold-out set would already be present in the training sets, thus leading to overfitting (James et al., 2013) .

The procedure for one iteration was as follows: The data was divided into a training (data of all participants except of one) and test set (just the left-out participant). All data from the training set went into CV2, where the data was split again in training and test sets in the same way. The algorithm learns the data structure from the training data, which means that the regression weights were estimated here. Afterwards, the prediction was performed on the left-out participant. In CV2 different possible lambdas were used in a randomized search to find the model with the smallest PE. The optimal lambda was then used in the LASSO PCR of CV1, which again involved model training and testing for the hold-out set. This whole procedure was repeated 32 times until each participant was in the test set of CV1 once. In the end, the PE was calculated based on the accuracy of all predictions in CV1.

Model performance

Two different criteria were used to assess model performance: the correlation of predicted and actual craving ratings and the PE (mean absolute deviation of predicted from observed craving ratings).

For validation of the model performance, a nonparametric permutation test (Nichols & Holmes, 2002) was applied. Here, craving ratings were permuted 1000 times and the cross-validated LASSO-PCR was repeated for each permuted dataset to obtain a distribution of the predicted and observed craving correlation. The mean of the permuted correlations should be symmetrically distributed around zero if the prediction is unbiased. In addition, the permuted PE and predicted-observed craving correlation should be significantly higher or respectively lower than the corresponding values of the correct data if the prediction is better than chance.

Visualization and interpretation

A bootstrap test (Efron & Tibshirani, 1993) was performed to threshold and visualize reliable voxels for interpretation of the prediction. 5000 bootstrap samples (with replacement) of paired contrast maps and craving ratings were collected, and the LASSO-PCR procedure was repeated for each one. Subsequently, two-tailed uncorrected p-values were computed for every voxel and False Discovery Rate correction (Benjamini & Hochberg, 1995) was applied. The test was based on the proportion of weights below or above zero in one voxel. This procedure allows to identify voxels that provide the most reliable contribution to the prediction (Wager et al., 2011). For visualization the regression weights were back-projected into voxel space to generate a 3D image of the brain.

Statistical analysis of behavioral ratings

Pearson’s correlation coefficient was employed to assess the association of behavioral craving and valence ratings.

Results

fMRI analysis

Cross-validated prediction of craving

The correlation of predicted and observed craving ratings was r = .01 (Figure 4). The average PE of the cross-validated LASSO-PCR was 13.00 (*SD* = 15.58; 100-point visual analog scale). The variance in craving ratings (outcome) explained by the weights (predictor) was less than 1% ($R^2 < .001$).

Figure 4

Scatterplot Showing Correlation of Predicted and Observed Craving

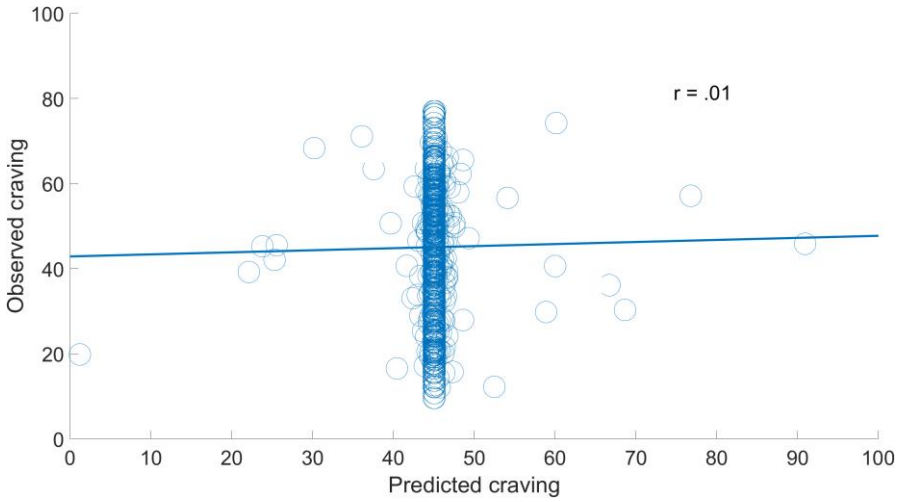

Model performance craving

Permuting the craving ratings 1000 times and repeating the cross-validated LASSO-PCR on each permuted dataset gave us a distribution of the correlation of predicted and observed ratings (Figure 5) and the PE (Figure 6). The procedure revealed that the mean of the permuted correlations, although symmetrically distributed around zero, was not significantly different from the true correlation (p = .83). Additionally, the permuted PE and the actual PE did not differ significantly (p = .66). Therefore, the ML model for predicting craving does not perform better than chance.

Figure 5

Distribution of Predicted and Observed Craving Correlation from Non-Parametric Permutation Test

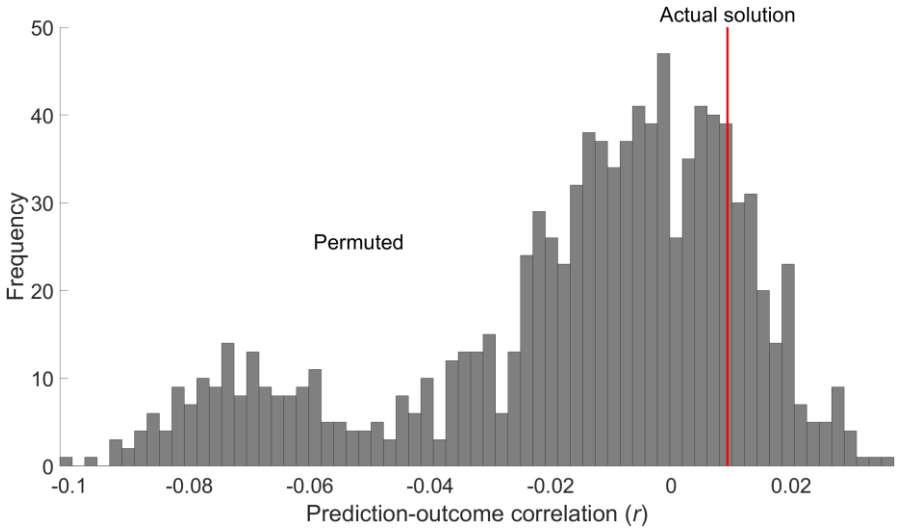

Figure 6

Distribution of Prediction Error for Craving from Non-Parametric Permutation Test

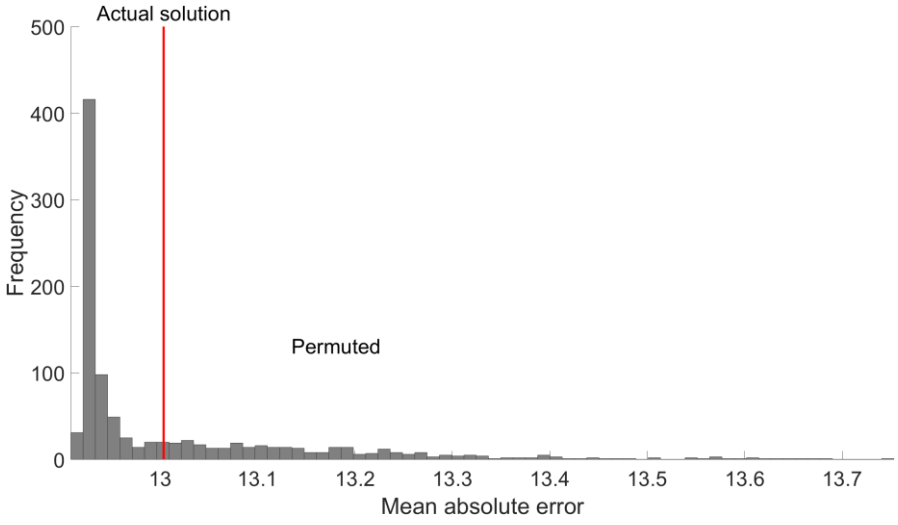

Bootstrapping & visualization craving

No predictive regression weights were found before and after thresholding via 5000 bootstrap samples in the cross-validated LASSO-PCR for craving, therefore no visualization was performed. The bootstrapped *p*-values for each voxel ranged between .76 and 1 (M = .88, SD = .08).

Cross-validated prediction of valence

The correlation of predicted and observed valence ratings was $r < .01$ (Figure 7). The average PE of the cross-validated LASSO-PCR was 7.02 (SD = 9.01; 100-point visual analog scale). The variance in valence ratings (outcome) explained by the weights (predictor) was less than 1% ($R^2 < .001$).

Figure 7

Scatterplot Showing Correlation of Predicted and Observed Valence

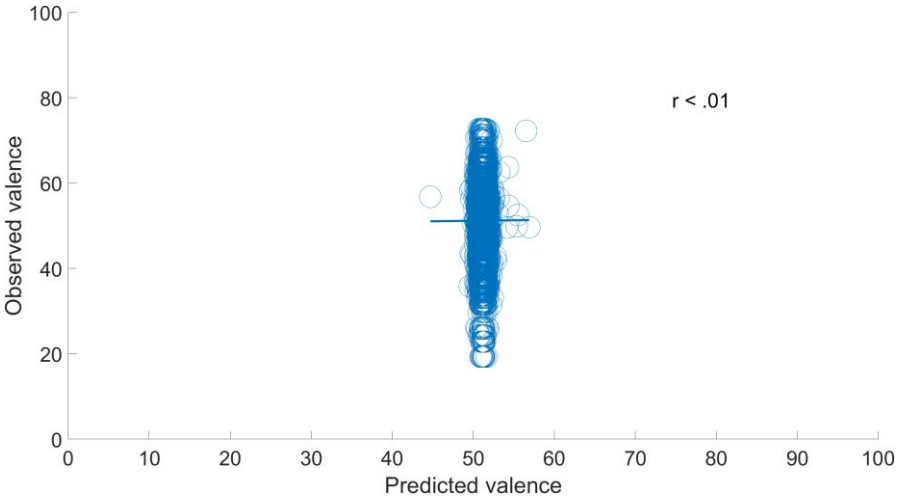

Model performance valence

Permuting the valence ratings 1000 times and repeating the cross-validated LASSO-PCR on each permuted dataset gave us a distribution of the correlation of predicted and observed ratings (Figure 8) and the PE (Figure 9). The procedure revealed that the mean of the permuted correlations, although symmetrically distributed around zero, was not significantly different from the true correlation (p = .68). Additionally, the permuted PE and the actual PE did not differ significantly (p = .51). Therefore, the ML model for predicting valence does not perform better than chance.

Figure 8

Distribution of Predicted and Observed Valence Correlation from Non-Parametric Permutation Test

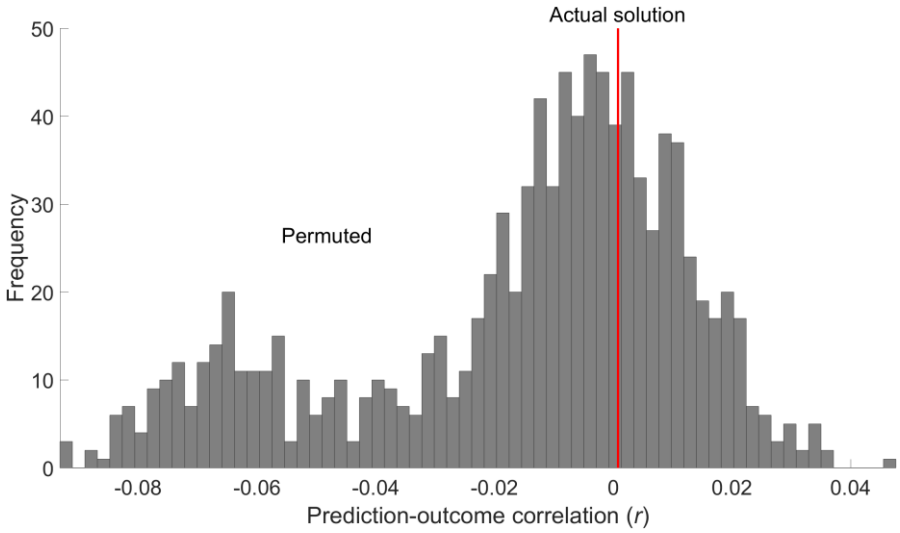

Figure 9

Distribution of Prediction Error for Valence from Non-Parametric Permutation Test

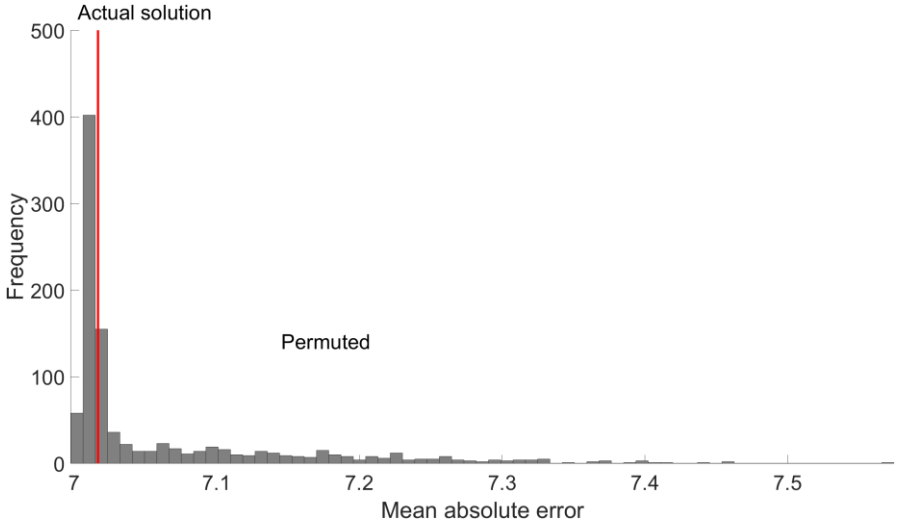

Bootstrapping & visualization valence

Low predictive regression weights near zero (> 0.001) were obtained in the cross-validated LASSO-PCR for valence, these were not found to be reliable after thresholding for interpretation via 5000 bootstrap samples (see Figure 10). The bootstrapped *p*-values for each voxel ranged between .63 and 1 (*M* = .84, *SD* = .09).

Figure 10

Predictive Voxel Weights for Valence Before and After Bootstrapping

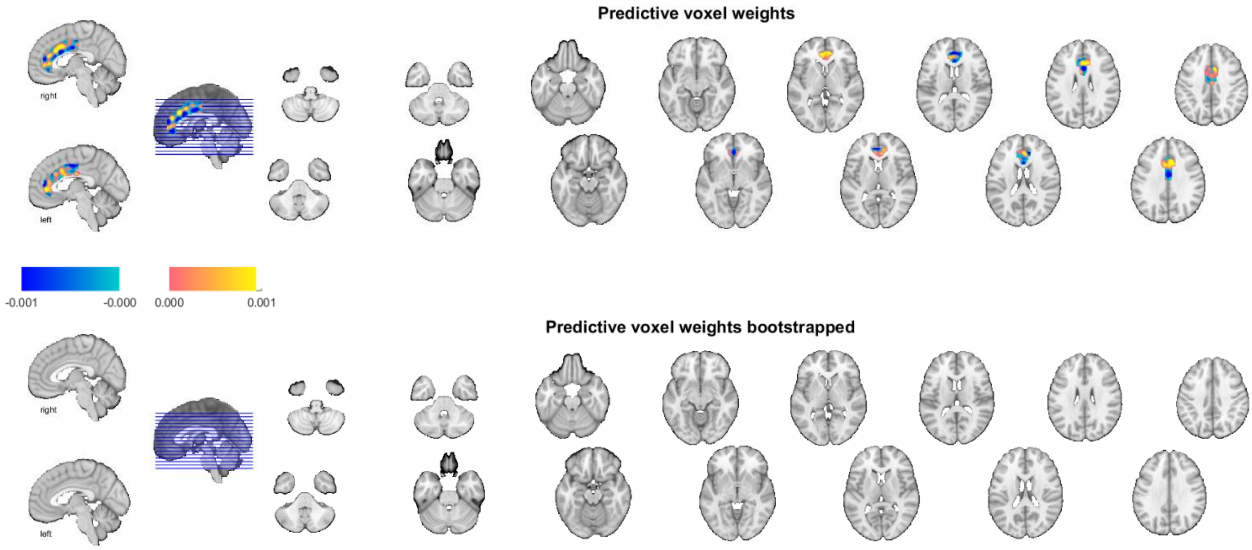

Note. Above: Unthresholded voxel weights obtained with LASSO-PCR for predicting valence. Below: No voxel weights remained significant after thresholding with bootstrap. Blue indicates negative predictive weights and yellow indicates positive predictive weights.

Behavioral craving and valence ratings

The ratings of craving (*M* = 45.10, *SD* = 15.78, *Median* = 46.99) and valence (*M* = 51.20, *SD* = 8.97, *Median* = 52.13) were significantly correlated (*r* = .72, *p* < .001; see Figure 11). The ratings were normally distributed around their respective means, this is shown in Figure 12 (craving) and Figure 13 (valence).

Figure 11

Scatterplot Showing Correlation of Behavioral Craving and Valence Ratings

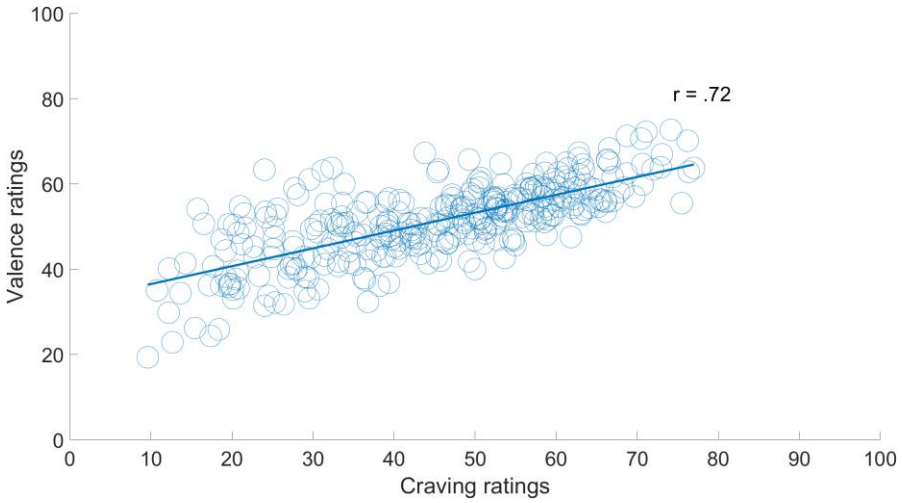

Figure 12

Distribution of Behavioral Craving Ratings in the Study (N = 32)

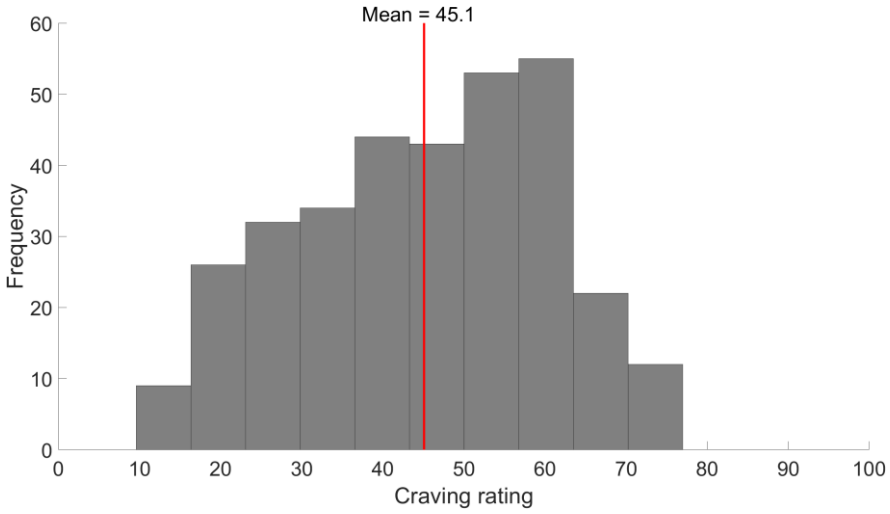

Figure 13

Distribution of Behavioral Valence Ratings in the Study (N = 32)

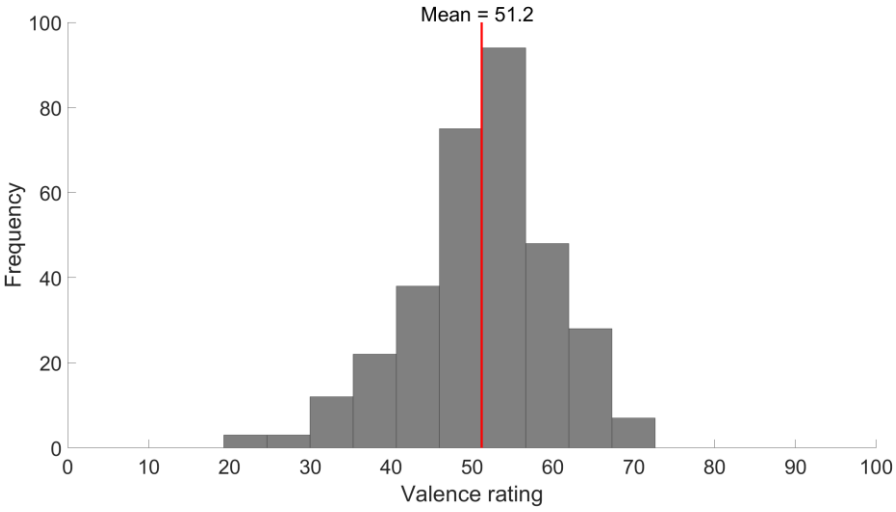

Discussion

The purpose of this study was to predict nicotine-related craving ratings in smokers from the ACC with a ML approach. In contrast, we hypothesized that the ML model would not predict valence ratings from the ACC. While previous studies mainly focused on spatial localization of brain regions involved in cigarette craving processing, we aimed to achieve a higher degree of brain activity quantification by predicting single-trial ratings. However, we found that the LASSO-PCR method we chose could not predict craving nor valence from BOLD activity in the ACC.

Predicting craving and valence

The outcome of the LASSO-PCR on craving ratings was not in line with results of standard GLM methods. Using GLM-based approaches, activity in the ACC has been found to be involved in cigarette craving in numerous studies (Brody et al., 2007; Canterberry et al., 2013; Kühn & Gallinat, 2011; Li et al., 2013). In contrast, the results on valence were as expected, as valence ratings seem to explain more variance of the activity in the amygdala, but not in the ACC, compared to arousal (Anders et al., 2008) or craving ratings (Haugg et al., 2021).

These previous approaches are fundamentally different from our method, in which we employed the LS-S approach (Mumford et al., 2012) for trial-by-trial deconvolution to generate contrast maps of brain activity that were used as input for the ML model. The LS-S approach is seen as the best method for estimating true neural activity in rapid event-related designs for multivariate fMRI analyses. However, its usefulness has only been tested for classification algorithms (Mumford et al., 2012) and not for regression models, as in the case of our study. Additionally, it was found that the benefit of LS-S decreases the shorter the inter-stimulus interval (ISI) is (Mumford et al., 2012). It appears that with smaller ISI the regressors (here the individual trials) correlate more strongly with each other, which negatively affects the model performance. Thereby, it was established that an ISI of 3 s is suitable for the application of LS-S without losing predictive accuracy (Mumford et al., 2014). However, an ISI of 2.3 was used in our study, as it was initially planned only for univariate analysis with a parametric modulator, for which it appeared to be appropriate (Haugg et al., 2021).

These findings on deconvolution methods only refer to multivariate analyses with classification models. Thus, there seems to be a literature gap regarding data preparation for regression algorithms and optimization of fMRI designs for this type of analysis. While classification models usually distinguish between two outcomes (classes), regression methods try

to predict continuous values. There are indeed examples of studies that successfully predicted continuous outcomes like arousal (Chu et al., 2011), placebo analgesia score (Wager et al., 2011), subjective physical pain (Wager et al., 2013), negative affect (Chang et al., 2015), or subjective fear (Taschereau-Dumouchel et al., 2020). However, some used other ML methods such as kernel ridge regression (Chu et al., 2011) or support vector regression (Taschereau-Dumouchel et al., 2020). Furthermore, all these studies examined whole-brain decoders, while we chose the ACC as region of interest. Most notably, all psychological ratings were acquired on a Likert scale with only five (Chang et al., 2015; Chu et al., 2011; Taschereau-Dumouchel et al., 2020; Wager et al., 2011) or nine (Wager et al., 2013) rating levels, while we tried to predict ratings acquired from a 0-100 scale. Although this is highly debated, differences in psychological scales could have introduced more uncertainty on the psychological dimension, which equates to more uncertainty on the ML target. This provides an additional explanation for the unexpected results. Consequently, the general ability to predict subjective ratings with a high number of levels should be explored in future studies.

Furthermore, we noted that the pattern of individual ratings in the first half of a rating session was different from the second half (for example images of the second half tended to be rated with equal urge and valence), which we interpreted as a decrease of the participant´s engagement in the rating task. We therefore capitalized on shared effects instead of individual effects by averaging the rating of each image across participants and used the averaged values as ML targets instead of individual ones. The use of averaged ratings seemed suitable for a classical GLM with ratings as parametric modulators (Haugg et al., 2021), but this may not be the case for single-trial analyses, where every trial matters individually. Hence, the quality of the ratings could further explain why our analysis was not successful. Moreover, craving and valence ratings were highly correlated with each other (r = .72), making it unlikely that they can be distinguished easily based on brain activity of a single region.

Another critical point is the relatively small sample size with 32 subjects. Classical power analyses for fMRI in combination with ML analyses appear to be not robust (Mumford, 2012). However, other studies using LASSO-PCR to predict continuous outcomes collected far more data with 70 (Wager et al., 2011) and 113 (Wager et al., 2013) subjects, for example. This indicates that our sample size was too small to successfully apply a ML method.

In summary, our unexpected outcome could be equally explained by unsuitable experimental design (low ISI), insufficient quality of the ML target (averaged versus individual

ratings) and type of the ML model itself. For this reason, it is important to mention that our study does not rule out the role of ACC activation in nicotine-related craving or valence in smokers but suggests that overall noise levels in our data were too high for the analysis to be successful.

Future directions

In our analysis, we attempted to find not only mere correlations between brain activity and cue-induced craving, but a more precise pattern at the level of single-trial predictions. There are treatments specifically designed to reduce craving in smokers to support smoking cessation, such as cue exposure therapy (Conklin & Tiffany, 2002; Drummond et al., 1990) and real-time fMRI neurofeedback (Cox et al., 1995; Sulzer et al., 2013). In cue exposure therapy, the patient is exposed to drug stimuli, which is intended to extinguish conditioned responses such as craving. Real-time neurofeedback in the context of nicotine addiction is designed to reduce cue-induced craving by helping individuals to voluntarily regulate the brain activity that is responsible for it. However, the efficacy of these treatments for smoking cessation remains unclear. There are empirical findings suggesting low efficacy of cue exposure therapy (Pericot-Valverde et al., 2019) and equality to treatments like cognitive behavioral therapy (Park et al., 2014), or providing contradictory results (Unrod et al., 2014). Similarly, with real-time fMRI neurofeedback, there are studies supporting the efficacy of this method (Hartwell et al., 2016; Li et al., 2013) or providing mixed results (Canterberry et al., 2013; Pandria et al., 2020). Thus, there remains room for improvement in these treatment options. Future research on cue-driven craving on a neurological level with multivariate approaches can increase the psychological specificity and overall accuracy of both interventions. For example, in targeting the specific craving component with smoking cues or in shaping the stimuli depending on the patients individual craving level.

Conclusion

This work aimed to predict behavioral craving ratings from fMRI BOLD activity, which was not possible with the chosen LASSO-PCR model. These results can be attributed to different factors: quality of the behavioral ratings, the chosen ML model, and an unsuitable experimental design (short ISI), indicating that event-related designs need to be adapted when this ML regression algorithm is used for single-trial prediction. However, studying cue-induced craving with multivariate methods is further important to improve treatments for smoking cessation. Overall, we hope to contribute to the optimization of experimental methods for this purpose.

References

Allenby, C., Falcone, M., Wileyto, E. P., Cao, W., Bernardo, L., Ashare, R. L., Janes, A., Loughead, J., & Lerman, C. (2020). Neural cue reactivity during acute abstinence predicts short-term smoking relapse. *Addiction Biology*, *25*(2). https://doi.org/10.1111/adb.12733

American Psychiatric Association. (2013). *Diagnostic and statistical manual of mental disorders* (5th ed.). American Psychiatric Association. https://doi.org/10.1176/appi.books.9780890425596

Anders, S., Eippert, F., Weiskopf, N., & Veit, R. (2008). The human amygdala is sensitive to the valence of pictures and sounds irrespective of arousal: An fMRI study. *Social Cognitive and Affective Neuroscience*, *3*(3), 233–243. https://doi.org/10.1093/scan/nsn017

Babb, S., Malarcher, A., Schauer, G., Asman, K., & Jamal, A. (2017). Quitting smoking among adults — United States, 2000–2015. *Morbidity and Mortality Weekly Report*, *65*(52), 1457–1464. https://www.jstor.org/stable/24876523

Bagot, K. S., Heishman, S. J., & Moolchan, E. T. (2007). Tobacco craving predicts lapse to smoking among adolescent smokers in cessation treatment. *Nicotine & Tobacco Research*, *9*(6), 647–652. https://doi.org/10.1080/14622200701365178

Baxter, M. G., & Murray, E. A. (2002). The amygdala and reward. *Nature Reviews Neuroscience*, *3*(7), 563–573. https://doi.org/10.1038/nrn875

Bellman, R. (2015). *Adaptive control processes*. Princeton University Press.

Benjamini, Y., & Hochberg, Y. (1995). Controlling the false discovery rate: a practical and powerful approach to multiple testing. *Journal of the Royal Statistical Society: Series B (Methodological)*, *57*(1), 289–300.

Betts, J. M., Dowd, A. N., Forney, M., Hetelekides, E., & Tiffany, S. T. (2021). A meta-analysis of cue reactivity in tobacco cigarette smokers. *Nicotine & Tobacco Research*, *23*(2), 249–258. https://doi.org/10.1093/ntr/ntaa147

Brody, A. L., Mandelkern, M. A., Olmstead, R. E., Jou, J., Tiongson, E., Allen, V., Scheibal, D., London, E. D., Monterosso, J. R., Tiffany, S. T., Korb, A., Gan, J. J., & Cohen, M. S. (2007). Neural substrates of resisting craving during cigarette cue exposure. *Biological Psychiatry*, *62*(6), 642–651. https://doi.org/10.1016/j.biopsych.2006.10.026

Bush, G., Vogt, B. A., Holmes, J., Dale, A. M., Greve, D., Jenike, M. A., & Rosen, B. R. (2002). Dorsal anterior cingulate cortex: A role in reward-based decision making. *Proceedings of the National Academy of Sciences*, *99*(1), 523–528. https://doi.org/10.1073/pnas.012470999

Canterberry, M., Hanlon, C. A., Hartwell, K. J., Li, X., Owens, M., LeMatty, T., Prisciandaro, J. J., Borckardt, J., Saladin, M. E., Brady, K. T., & George, M. S. (2013). Sustained reduction of nicotine craving with real-time neurofeedback: Exploring the role of severity of dependence. *Nicotine & Tobacco Research*, *15*(12), 2120–2124. https://doi.org/10.1093/ntr/ntt122

Carter, B. L., & Tiffany, S. T. (1999). Meta-analysis of cue-reactivity in addiction research. *Addiction*, *94*(3), 327–340. https://doi.org/10.1046/j.1360-0443.1999.9433273.x

Chang, L. J., Gianaros, P. J., Manuck, S. B., Krishnan, A., & Wager, T. (2015). A sensitive and

specific neural signature for picture-induced negative affect. *PLOS Biology*, *13*(6), e1002180. https://doi.org/10.1371/journal.pbio.1002180

Chase, H. W., Eickhoff, S. B., Laird, A. R., & Hogarth, L. (2011). The neural basis of drug stimulus processing and craving: An activation likelihood estimation meta-analysis. *Biological Psychiatry*, *70*(8), 785–793. https://doi.org/10.1016/j.biopsych.2011.05.025

Chu, C., Ni, Y., Tan, G., Saunders, C. J., & Ashburner, J. (2011). Kernel regression for fMRI pattern prediction. *NeuroImage*, *56*(2), 662–673. https://doi.org/10.1016/j.neuroimage.2010.03.058

Conklin, C. A., & Tiffany, S. T. (2002). Applying extinction research and theory to cue-exposure addiction treatments. *Addiction*, *97*(2), 155–167. https://doi.org/10.1046/j.1360-0443.2002.00014.x

Costafreda, S. G., Brammer, M. J., David, A. S., & Fu, C. H. Y. (2008). Predictors of amygdala activation during the processing of emotional stimuli: A meta-analysis of 385 PET and fMRI studies. *Brain Research Reviews*, *58*(1), 57–70. https://doi.org/10.1016/j.brainresrev.2007.10.012

Cox, R. W., Jesmanowicz, A., & Hyde, J. S. (1995). Real-time functional magnetic resonance imaging. *Magnetic Resonance in Medicine*, *33*(2), 230–236. https://doi.org/10.1002/mrm.1910330213

Daniel, R., & Pollmann, S. (2014). A universal role of the ventral striatum in reward-based learning: Evidence from human studies. *Neurobiology of Learning and Memory*, *114*, 90–100. https://doi.org/10.1016/j.nlm.2014.05.002

Drummond, D., Cooper, T., & Glautier, S. (1990). Conditioned learning in alcohol dependence: implications for cue exposure treatment. *Addiction*, *85*(6), 725–743. https://doi.org/10.1111/j.1360-0443.1990.tb01685.x

Drummond, D., Tiffany, S. T., Glautier, S., & Remington, B. (1995). Cue exposure in understanding and treating addictive behaviours. In D. Drummond, S. T. Tiffany, S. Glautier, & B. Remington (Eds.), *Addictive behaviour: Cue exposure theory and practice* (pp. 1–17). John Wiley & Sons.

Efron, B., & Tibshirani, R. J. (1993). *An introduction to the bootstrap*. Springer US. https://doi.org/10.1007/978-1-4899-4541-9

Eissenberg, T. (2004). Measuring the emergence of tobacco dependence: The contribution of negative reinforcement models. *Addiction*, *99*, 5–29. https://doi.org/10.1111/j.1360-0443.2004.00735.x

Elfeddali, I., Bolman, C., Candel, M. J. J. M., Wiers, R. W., & De Vries, H. (2012). The role of self-efficacy, recovery self-efficacy, and preparatory planning in predicting short-term smoking relapse. *British Journal of Health Psychology*, *17*(1), 185–201. https://doi.org/10.1111/j.2044-8287.2011.02032.x

Ferguson, S. G., & Shiffman, S. (2009). The relevance and treatment of cue-induced cravings in tobacco dependence. *Journal of Substance Abuse Treatment*, *36*(3), 235–243. https://doi.org/10.1016/j.jsat.2008.06.005

Gallagher, M., & Chiba, A. A. (1996). The amygdala and emotion. *Current Opinion in Neurobiology*, *6*(2), 221–227. https://doi.org/10.1016/S0959-4388(96)80076-6

García-Rodríguez, O., Secades-Villa, R., Flórez-Salamanca, L., Okuda, M., Liu, S.-M., & Blanco, C. (2013). Probability and predictors of relapse to smoking: Results of the National Epidemiologic Survey on Alcohol and Related Conditions (NESARC). *Drug and Alcohol Dependence*, *132*(3), 479–485. https://doi.org/10.1016/j.drugalcdep.2013.03.008

Gilbert, D. G., & Rabinovich, N. E. (1999). *International Smoking Images Series Version 1.2.*

Gottfried, J. A., O'Doherty, J., & Dolan, R. (2003). Encoding predictive reward value in human amygdala and orbitofrontal cortex. *Science*, *301*(5636), 1104–1107. https://doi.org/10.1126/science.1087919

Hartmann-Boyce, J., Chepkin, S. C., Ye, W., Bullen, C., & Lancaster, T. (2018). Nicotine replacement therapy versus control for smoking cessation. *Cochrane Database of Systematic Reviews*, *2019*(1). https://doi.org/10.1002/14651858.CD000146.pub5

Hartwell, K. J., Hanlon, C. A., Li, X., Borckardt, J. J., Canterberry, M., Prisciandaro, J. J., Moran-Santa Maria, M. M., LeMatty, T., George, M. S., & Brady, K. T. (2016). Individualized real-time fMRI neurofeedback to attenuate craving in nicotine-dependent smokers. *Journal of Psychiatry & Neuroscience*, *41*(1), 48–55. https://doi.org/10.1503/jpn.140200

Hastie, T., Tibshirani, R., & Friedman, J. (2009). *The elements of statistical learning*. Springer New York. https://doi.org/10.1007/978-0-387-84858-7

Haugg, A., Manoliu, A., Sladky, R., Hulka, L. M., Kirschner, M., Brühl, A. B., Seifritz, E., Quednow, B. B., Herdener, M., & Scharnowski, F. (2021). Disentangling craving- and valence-related brain responses to smoking cues in individuals with nicotine use disorder. *Addiction Biology*. https://doi.org/10.1111/adb.13083

Haxby, J. V. (2012). Multivariate pattern analysis of fMRI: The early beginnings. *NeuroImage*, *62*(2), 852–855. https://doi.org/10.1016/j.neuroimage.2012.03.016

Haynes, J.-D., & Rees, G. (2006). Decoding mental states from brain activity in humans. *Nature Reviews Neuroscience*, *7*(7), 523–534. https://doi.org/10.1038/nrn1931

Heatherton, T. F., Kozlowski, L. T., Frecker, R. C., & Fagerstrom, K.-O. (1991). The Fagerstrom Test for nicotine dependence: A revision of the Fagerstrom Tolerance Questionnaire. *Addiction*, *86*(9), 1119–1127. https://doi.org/10.1111/j.1360-0443.1991.tb01879.x

Hughes, J. R. (1992). Tobacco withdrawal in self-quitters. *Journal of Consulting and Clinical Psychology*, *60*(5), 689–697. https://doi.org/10.1037/0022-006X.60.5.689

James, G., Witten, D., Hastie, T., & Tibshirani, R. (2013). *An introduction to statistical learning* (Vol. 103). Springer New York. https://doi.org/10.1007/978-1-4614-7138-7

Janes, A. C., Pizzagalli, D. A., Richardt, S., Frederick, B. deB., Chuzi, S., Pachas, G., Culhane, M. A., Holmes, A. J., Fava, M., Evins, A. E., & Kaufman, M. J. (2010). Brain reactivity to smoking cues prior to smoking cessation predicts ability to maintain tobacco abstinence. *Biological Psychiatry*, *67*(8), 722–729. https://doi.org/10.1016/j.biopsych.2009.12.034

Kalivas, P. W., & Volkow, N. D. (2005). The neural basis of addiction: A pathology of motivation and choice. *American Journal of Psychiatry*, *162*(8), 1403–1413. https://doi.org/10.1176/appi.ajp.162.8.1403

Killen, J. D., & Fortmann, S. P. (1997). Craving is associated with smoking relapse: Findings from three prospective studies. *Experimental and Clinical Psychopharmacology*, *5*(2), 137–142. https://doi.org/10.1037/1064-1297.5.2.137

Kohavi, R. (1995). A study of cross-validation and bootstrap for accuracy estimation and model selection. *International Joint Conference on Artificial Intelligence*, *14*(2), 1137–1145.

Kühn, S., & Gallinat, J. (2011). Common biology of craving across legal and illegal drugs - a quantitative meta-analysis of cue-reactivity brain response. *European Journal of Neuroscience*, *33*(7), 1318–1326. https://doi.org/10.1111/j.1460-9568.2010.07590.x

Lancaster, T., & Stead, L. F. (2017). Individual behavioural counselling for smoking cessation. *Cochrane Database of Systematic Reviews*, *2018*(3). https://doi.org/10.1002/14651858.CD001292.pub3

Lang, P. J., Bradley, M. M., & Cuthbert, B. N. (1997). International affective picture system (IAPS): Technical manual and affective ratings. *NIMH Center for the Study of Emotion and Attention*, *1*, 39–58.

Li, X., Hartwell, K. J., Borckardt, J., Prisciandaro, J. J., Saladin, M. E., Morgan, P. S., Johnson, K. A., LeMatty, T., Brady, K. T., & George, M. S. (2013). Volitional reduction of anterior cingulate cortex activity produces decreased cue craving in smoking cessation: A preliminary real-time fMRI study. *Addiction Biology*, *18*(4), 739–748. https://doi.org/10.1111/j.1369-1600.2012.00449.x

Manoliu, A., Haugg, A., Sladky, R., Hulka, L., Kirschner, M., Brühl, A. B., Seifritz, E., Quednow, B., Herdener, M., & Scharnowski, F. (2021). SmoCuDa: A validated smoking cue database to reliably induce craving in tobacco use disorder. *European Addiction Research*, *27*(2), 107–114. https://doi.org/10.1159/000509758

Mumford, J. A. (2012). A power calculation guide for fMRI studies. *Social Cognitive and Affective Neuroscience*, *7*(6), 738–742. https://doi.org/10.1093/scan/nss059

Mumford, J. A., Davis, T., & Poldrack, R. A. (2014). The impact of study design on pattern estimation for single-trial multivariate pattern analysis. *NeuroImage*, *103*, 130–138. https://doi.org/10.1016/j.neuroimage.2014.09.026

Mumford, J. A., Turner, B. O., Ashby, F. G., & Poldrack, R. A. (2012). Deconvolving BOLD activation in event-related designs for multivoxel pattern classification analyses. *NeuroImage*, *59*(3), 2636–2643. https://doi.org/10.1016/j.neuroimage.2011.08.076

Nakajima, M., & Al'Absi, M. (2012). Predictors of risk for smoking relapse in men and women: A prospective examination. *Psychology of Addictive Behaviors*, *26*(3), 633–637. https://doi.org/10.1037/a0027280

Nichols, T. E., & Holmes, A. P. (2002). Nonparametric permutation tests for functional neuroimaging: A primer with examples. *Human Brain Mapping*, *15*(1), 1–25. https://doi.org/10.1002/hbm.1058

Nieva, G., Valero, S., Bruguera, E., Andión, Ó., Trasovares, M. V., Gual, A., & Casas, M. (2011). The alternative five-factor model of personality, nicotine dependence and relapse after treatment for smoking cessation. *Addictive Behaviors*, *36*(10), 965–971. https://doi.org/10.1016/j.addbeh.2011.05.008

Pandria, N., Athanasiou, A., Konstantara, L., Karagianni, M., & Bamidis, P. D. (2020). Advances in biofeedback and neurofeedback studies on smoking. *NeuroImage: Clinical*, *28*(May), 102397. https://doi.org/10.1016/j.nicl.2020.102397

Park, C.-B., Choi, J.-S., Park, S. M., Lee, J.-Y., Jung, H. Y., Seol, J.-M., Hwang, J. Y., Gwak, A. R., & Kwon, J. S. (2014). Comparison of the effectiveness of virtual cue exposure therapy and cognitive behavioral therapy for nicotine dependence. *Cyberpsychology, Behavior, and Social Networking*, *17*(4), 262–267. https://doi.org/10.1089/cyber.2013.0253

Pavlov, I. P. (1927). *Conditioned reflexes: An investigation of the physiological activity of the cerebral cortex*. Oxford University Press.

Pericot-Valverde, I., Secades-Villa, R., & Gutiérrez-Maldonado, J. (2019). A randomized clinical trial of cue exposure treatment through virtual reality for smoking cessation. *Journal of Substance Abuse Treatment*, *96*, 26–32. https://doi.org/10.1016/j.jsat.2018.10.003

Potvin, S., Tikàsz, A., Dinh-Williams, L. L.-A., Bourque, J., & Mendrek, A. (2015). Cigarette cravings, impulsivity, and the brain. *Frontiers in Psychiatry*, *6*. https://doi.org/10.3389/fpsyt.2015.00125

Powell, J., Dawkins, L., West, R., Powell, J., & Pickering, A. (2010). Relapse to smoking during unaided cessation: Clinical, cognitive and motivational predictors. *Psychopharmacology*, *212*(4), 537–549. https://doi.org/10.1007/s00213-010-1975-8

Quednow, B. B., & Herdener, M. (2016). *Human pharmacology for addiction medicine* (pp. 227–250). https://doi.org/10.1016/bs.pbr.2015.07.017

Quednow, B. B., Kühn, K.-U., Hoenig, K., Maier, W., & Wagner, M. (2004). Prepulse inhibition and habituation of acoustic startle response in male MDMA (‘Ecstasy’) users, cannabis users, and healthy controls. *Neuropsychopharmacology*, *29*(5), 982–990. https://doi.org/10.1038/sj.npp.1300396

Robinson, T., & Berridge, K. (1993). The neural basis of drug craving: An incentive-sensitization theory of addiction. *Brain Research Reviews*, *18*(3), 247–291. https://doi.org/10.1016/0165-0173(93)90013-P

Samet, J. M. (2013). Tobacco smoking. *Thoracic Surgery Clinics*, *23*(2), 103–112. https://doi.org/10.1016/j.thorsurg.2013.01.009

Sanderson Cox, L., Tiffany, S., & Christen, A. (2001). Evaluation of the brief questionnaire of smoking urges (QSU-brief) in laboratory and clinical settings. *Nicotine & Tobacco Research*, *3*(1), 7–16. https://doi.org/10.1080/14622200124218

Schoenbaum, G., Roesch, M. R., & Stalnaker, T. A. (2006). Orbitofrontal cortex, decision-making and drug addiction. *Trends in Neurosciences*, *29*(2), 116–124. https://doi.org/10.1016/j.tins.2005.12.006

See, R. E., Fuchs, R. A., Ledford, C. C., & McLaughlin, J. (2006). Drug addiction, relapse, and

the amygdala. *Annals of the New York Academy of Sciences*, *985*(1), 294–307. https://doi.org/10.1111/j.1749-6632.2003.tb07089.x

Simmonds, D. J., Pekar, J. J., & Mostofsky, S. H. (2008). Meta-analysis of go/no-go tasks demonstrating that fMRI activation associated with response inhibition is task-dependent. *Neuropsychologia*, *46*(1), 224–232. https://doi.org/10.1016/j.neuropsychologia.2007.07.015

Skinner, B. F. (1963). Operant behavior. *American Psychologist*, *18*(8), 503–515. https://doi.org/10.1037/h0045185

Sulzer, J., Haller, S., Scharnowski, F., Weiskopf, N., Birbaumer, N., Blefari, M. L., Bruehl, A. B., Cohen, L. G., DeCharms, R. C., Gassert, R., Goebel, R., Herwig, U., LaConte, S., Linden, D., Luft, A., Seifritz, E., & Sitaram, R. (2013). Real-time fMRI neurofeedback: progress and challenges. *NeuroImage*, *76*, 386–399. https://doi.org/10.1016/j.neuroimage.2013.03.033

Tang, D. W., Fellows, L. K., Small, D. M., & Dagher, A. (2012). Food and drug cues activate similar brain regions: A meta-analysis of functional MRI studies. *Physiology & Behavior*, *106*(3), 317–324. https://doi.org/10.1016/j.physbeh.2012.03.009

Taschereau-Dumouchel, V., Kawato, M., & Lau, H. (2020). Multivoxel pattern analysis reveals dissociations between subjective fear and its physiological correlates. *Molecular Psychiatry*, *25*(10), 2342–2354. https://doi.org/10.1038/s41380-019-0520-3

Tibshirani, R. (1996). Regression shrinkage and selection via the lasso. *Journal of the Royal Statistical Society: Series B (Methodological)*, *58*(1), 267–288.

Tiffany, S. T. (1990). A cognitive model of drug urges and drug-use behavior: Role of automatic and nonautomatic processes. *Psychological Review*, *97*(2), 147–168. https://doi.org/10.1037/0033-295X.97.2.147

Tiffany, S. T. (1995). The role of cognitive factors in reactivity to drug cues. In *Addictive behaviour: Cue exposure theory and practice.* (pp. 137–165). John Wiley & Sons.

Tong, C., Bovbjerg, D. H., & Erblich, J. (2007). Smoking-related videos for use in cue-induced craving paradigms. *Addictive Behaviors*, *32*(12), 3034–3044. https://doi.org/10.1016/j.addbeh.2007.07.010

Unrod, M., Drobes, D. J., Stasiewicz, P. R., Ditre, J. W., Heckman, B., Miller, R. R., Sutton, S. K., & Brandon, T. H. (2014). Decline in cue-provoked craving during cue exposure therapy for smoking cessation. *Nicotine & Tobacco Research*, *16*(3), 306–315. https://doi.org/10.1093/ntr/ntt145

Wager, T. (2021). *CanlabCore, GitHub*. https://github.com/canlab/CanlabCore

Wager, T., Atlas, L. Y., Leotti, L. A., & Rilling, J. K. (2011). Predicting individual differences in placebo analgesia: Contributions of brain activity during anticipation and pain experience. *Journal of Neuroscience*, *31*(2), 439–452. https://doi.org/10.1523/JNEUROSCI.3420-10.2011

Wager, T., Atlas, L. Y., Lindquist, M. A., Roy, M., Woo, C.-W., & Kross, E. (2013). An fMRI-based neurologic signature of physical pain. *New England Journal of Medicine*, *368*(15), 1388–1397. https://doi.org/10.1056/NEJMoa1204471

Whitfield-Gabrieli, S., & Nieto-Castanon, A. (2012). Conn: A functional connectivity toolbox for correlated and anticorrelated brain networks. *Brain Connectivity*, *2*(3), 125–141. https://doi.org/10.1089/brain.2012.0073

World Health Organization. (2021). *WHO report on the global tobacco epidemic 2021*.

List of figures

List of abbreviations

ACC	Anterior cingulate cortex
BOLD	Blood oxygen level-dependent
CV	Cross-validation
DSM-V	Diagnostic and Statistical Manual of Mental Disorders 5th Edition
GLM	General linear model
fMRI	Functional magnetic resonance imaging
ISI	Inter-stimulus interval
LASSO-PCR	Least absolute shrinkage and selection operator-regularized principal component regression
LS-S	Least Squares-Separate
ML	Machine learning
PCA	Principal component analysis
PE	Prediction error

Deutsche Zusammenfassung

Nikotinabhängigkeit ist weltweit eine der Hauptursachen für vermeidbare Todesfälle und verursacht hohe Kosten für die Gesundheitssysteme. Leider sind die Rückfallquoten nach der Raucherentwöhnung hoch, so dass verbesserte Behandlungsmöglichkeiten erforderlich sind. Um neue wirksame Behandlungen anbieten zu können, ist ein tieferes Verständnis der zugrunde liegenden neuronalen und verhaltensbezogenen Mechanismen von Nikotinabhängigkeit erforderlich. Was die neuronalen Grundlagen der Nikotinsucht betrifft, so fand eine aktuelle Studie, dass die Aktivität im anterioren cingulären Kortex in erster Linie mit dem von externen Reizen ausgelösten Nikotinverlangen (Craving) zusammenhängt, während die Amygdala-Aktivität mit Valenzaspekten von Nikotinreizen in Verbindung gebracht wird. Diese Arbeit untersuchte eine mögliche Konfundierung von Valenz und Craving mit Hilfe eines Reiz-Reaktivitäts-Paradigmas. 32 nikotinabhängige Probanden unterzogen sich einer funktionellen Magnetresonanztomographie, während sie Craving-auslösende Bilder sahen, und bewerteten diese anschließend auf einer kontinuierlichen Skala in Bezug auf Craving und emotionale Valenz. Ein Modell des maschinellen Lernens (LASSO-PCR) wurde angewandt, um aus der neuronalen Aktivität im anterioren cingulären Kortex die Bewertungen der einzelnen Bildpräsentationen vorherzusagen. Wir gingen davon aus, dass nur die Craving-Bewertungen erfolgreich vorhergesagt werden können, aber es war weder möglich Craving noch Valenz korrekt vorherzusagen. Diese Ergebnisse können auf verschiedene Faktoren zurückgeführt werden: Qualität der Bewertungen, ungeeignete Interstimulus-Intervalle und das Modell selbst. Insgesamt ist die Optimierung von experimentellen Designs für multivariate Regressionsmethoden von großer Bedeutung, um die Forschung zum Reiz-bezogenen Craving bei Rauchern zu verbessern und damit gezieltere Behandlungsmöglichkeiten für die Raucherentwöhnung zu entwickeln.

Keywords: Craving, Reiz-Reaktivität, Nikotinabhängigkeit, funktionelle Magnetresonanztomographie, maschinelles Lernen

Acknowledgments

First of all, I would like to thank Cindy Lor for her great support. Without your knowledge, guidance and commitment, this thesis would not have been possible. Furthermore, I would like to thank Prof. Dr. Frank Scharnowski, who, despite difficult pandemic circumstances, accepted me into his group to realize this project and guided the whole process. And I also would like to thank Dr. David Steyrl for his machine learning advice.

Lastly, I am very grateful to my family and friends for their love and support during the last months.